

$$E_x = \frac{1}{2}t(\exp(ik_0n_Rz) + \exp(ik_0n_Lz)), \quad (4)$$

$$E_y = \frac{i}{2}t(\exp(ik_0n_Rz) - \exp(ik_0n_Lz)). \quad (5)$$

By simple algebraic manipulations, from Eq. (4) and (5) we derive

$$n_R = -\frac{i}{k_0} \frac{\Delta \ln(E_x - iE_y)}{\Delta z}, \quad (6)$$

$$n_L = -\frac{i}{k_0} \frac{\Delta \ln(E_x + iE_y)}{\Delta z}. \quad (7)$$

These formulas are essential for the WPRMC. In practice, the electric field is highly inhomogeneous inside the MTM unit cell, so we should use the volume averaged field. Bloch impedance Z_B (see the relevant discussion in review [18]) is retrieved unambiguously from the single reflection R on the vacuum–chiral MTM interface $Z_B = (1 + R)/(1 - R)$. Other EPs can be restored in the following conventional way: refractive index $n = (n_R + n_L)/2$, chirality $\kappa = (n_R - n_L)/2$.

Strictly speaking, the complex logarithm in Eqs. (6) and (7) is a multivalued function, so we can find the values of $i \ln(E_x \pm E_y)$ with accuracy up to $\pm 2\pi m$, where m is an integer. In order to apply a linear fit while using Eqs. (6) and (7), the dependence of $\text{Re}[i \ln(E_x \pm E_y)]$ on the unit cells coordinates z_{UC} should be made continuous. If the metamaterial is quasi-homogeneous the difference of the wave phase between neighboring unit cells should be less than $\pi/2$, thus aforementioned continuity is easy to persuade.

The constraints of the WPRMC are the same as of the WPRM for linearly polarized waves [17]. First, a metamaterial slab should be thick enough to prevent the reflection from the rear interface and standing wave formation. We found less than 1% error for the WPRM when $-45 < n'k_0d < 45$ and $5 < n''k_0d < 56$, where d is the slab thickness. For the case of low absorption, one can always increase d . Another option is to use a time-domain method and to terminate the simulation when the excitation pulse reaches the rear interface of the slab. Second, the accuracy of the simulations should be sufficient to observe the linear dependence of $i \ln(E_x \pm E_y)$ on the coordinate z , for that the electric field doesn't have to drop down to the noise level within less than three unit cells.

3. Case studies

To check the validity of the WPRMC and illustrate its application we consider 3 case studies: 1) homogeneous gyrotropic medium, 2) bi-cross MTM and 3) U-shaped MTM. Commercial software CST Microwave Studio [19] was used in simulations. Simulations were performed in the frequency domain with open boundary conditions in the direction of propagation and periodic boundary conditions in the lateral directions.

3.1 Homogeneous magnetized plasma

The main criteria for the WPRMC employment is that eigenwaves of the material are RCP and LCP waves, so this means that WPRMC is applicable to any material having circularly polarized eigenwaves. As a first example we chose homogeneous plasma magnetized along the direction of the wave propagation z . We should note that such medium is not a chiral medium, but its effective refractive index can be calculated analytically, so it is a reliable reference. Its permittivity tensor is $\boldsymbol{\varepsilon} = [(\varepsilon_1, i\varepsilon_2, 0), (-i\varepsilon_2, \varepsilon_1, 0), (0, 0, \varepsilon_3)]$, where

$$\varepsilon_1 = \varepsilon_\infty - \frac{\omega_p^2(\omega + i\omega_{COL})/\omega}{(\omega + i\omega_{COL})^2 - \omega_C^2}, \quad \varepsilon_2 = \frac{-\omega_p^2\omega_C/\omega}{(\omega + i\omega_{COL})^2 - \omega_C^2}, \quad \text{and} \quad \varepsilon_3 = \varepsilon_\infty - \frac{\omega_p^2}{\omega(\omega + i\omega_{COL})}.$$

The eigenwaves are RCP and LCP with refractive indices $n_R = (\varepsilon_1 + \varepsilon_2)^{1/2}$ and $n_L = (\varepsilon_1 - \varepsilon_2)^{1/2}$ [20]. For the simulations we chose plasma frequency $\omega_p = 1.0 \times 10^{15} s^{-1}$, cyclotron and collision frequencies $\omega_C = \omega_{COL} = 3.8 \times 10^{14} s^{-1}$ and $\varepsilon_\infty = 3$. For the simulation the slab of the plasma medium was divided into 100 layers. The WPRMC restores EPs in perfect agreement with the analytical ones (Fig. 1).

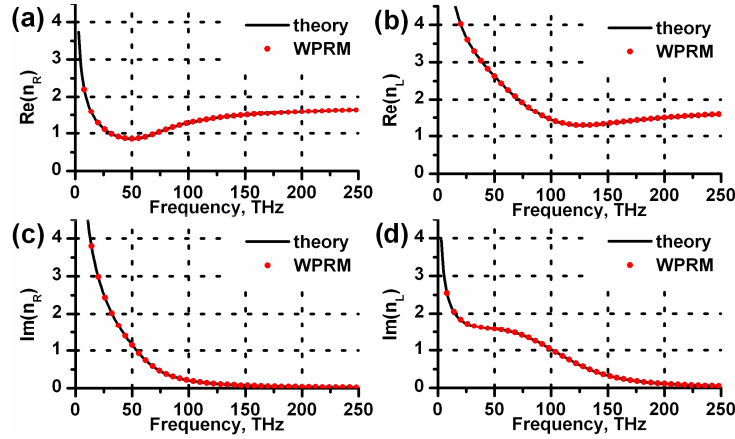


Fig. 1. (Color online). Theoretical (black line) and restored with WPRMC (red circles) refractive indices for RCP and LCP for the homogeneous magnetized plasma: (a) $\text{Re}(n_R)$, (b) $\text{Re}(n_L)$, (c) $\text{Im}(n_R)$, (d) $\text{Im}(n_L)$.

3.2 Bi-cross metamaterial

As the second example we investigated a slightly modified bi-cross metamaterial [21], that is a chiral metamaterial for the optical range. The geometrical parameters are indicated in Fig. 2. The crosses in the bi-cross are connected in the middle with a cylindrical conducting rod. The bi-cross material is silver, which is approximated as the Drude metal with plasma frequency $\omega_p = 1.37 \times 10^{16} s^{-1}$ and collision frequency $\omega_{COL} = 8.5 \times 10^{13} s^{-1}$ [22]. The silver structure is embedded into silica (refractive index $n = 1.44$).

In this case we lack the analytical results. Therefore WPRMC results are challenged against the ones, obtained by the standard method [15] as a reference. As we have already emphasized in the Introduction the EPs of few MTM layers are not the same as the bulk EPs so we do not anticipate the coincidence of the SM and WPRMC results. We have in mind rather the convergence of the SM results to WPRMC with the increasing thickness of the slab.

Indeed, the effective refractive indices converge very fast with the increase of the number of MTM layers (slab thickness) (Fig. 3). The effective properties of 3 layers are similar to the bulk ones restored with WPRMC from simulations of the 36 layers-thick structure.

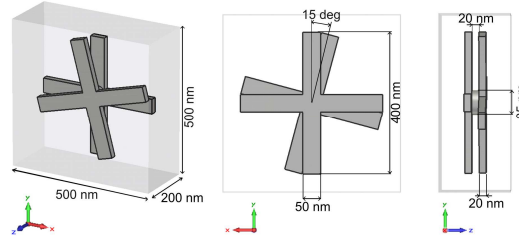


Fig. 2. (Color online). Connected bi-cross unit cell design and its geometrical parameters.

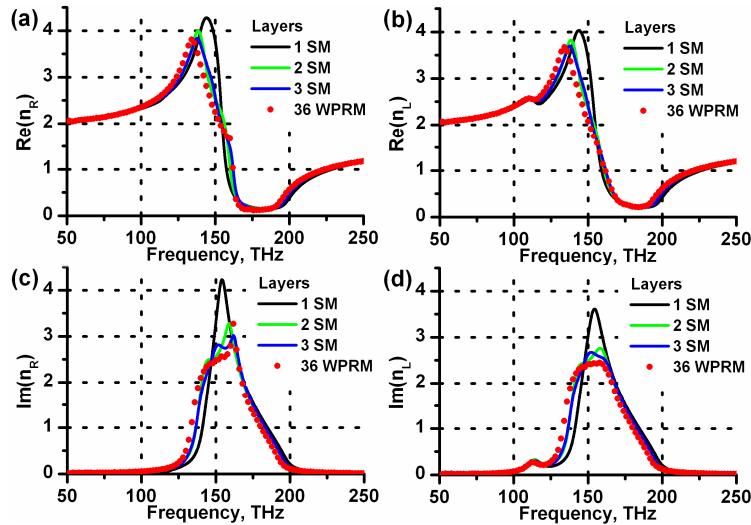


Fig. 3. (Color online). Effective refractive indices of the connected bi-cross MTM, retrieved with SM (one layer – black line, two layers – green line, three layers – blue line) and WPRM (red circles): (a) $\text{Re}(n_R)$, (b) $\text{Re}(n_L)$, (c) $\text{Im}(n_R)$, (d) $\text{Im}(n_L)$.

To further illustrate the restoration procedure we plotted the logarithm of the electric field amplitude dependence on the distance (layer number) inside the MTM slab (Fig. 4) for two different cases. At frequency 110 THz (Fig. 4a) the RCP and LCP waves have small absorption, but the MTM exhibits strong circular dichroism. We clearly see the standing wave after the layer number 20, so for retrieving we should use data points before that. At frequency 150 THz (Fig. 4b) absorption of both modes is high (and equal). We observe linear behavior of the field until the 19th layer then the wave amplitude is reaching the noise level. In this case, the last part should be excluded when applying Eqs. (6) and (7) for restoration.

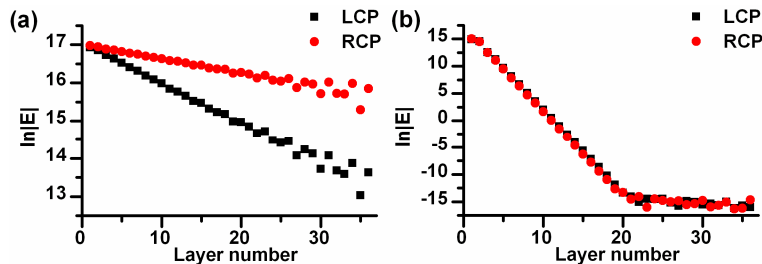


Fig. 4. (Color online). Logarithm of the electric field amplitude inside the bi-cross MTM slab at frequencies 110 THz (a) and 150 THz (b) for RCP (red circles) and LCP (black squares).

3.3 U-shaped metamaterial

To test our method in the microwave range we chose the recently published U-shaped metamaterial design [23]. The original paper presents the structure consisting of only two layers of MTM, so we stacked multiple layers for the WPRMC application (Fig. 5a). All the geometrical and material parameters were taken as in [23]. U-shaped resonators in each layer are 90 degrees rotated around their centers with respect to the preceding layer.

As we see from Fig. 5b and 5c, the effective properties change dramatically with the increasing thickness. One bi-layer of the U-shaped MTM shows pronounced negative values of the refractive index real part. For two bi-layers the refractive index is just slightly negative and further it becomes progressively positive for a thick structure (24 bi-layers). We explain this behavior as the result of strong interaction between meta-atoms in the adjacent layers, similar to the one described recently in [24]. Such interaction leads to mutual annihilation of total response finishing with a rather mitigated resonance. It is encouraging that correspondingly the absorption is much smaller than that of a single bi-layer (Fig. 5d and 5e). We suspect that the strong coupling between meta-atoms can represent a problem for the construction of bulk MTM on the basis of most of the proposed chiral MTMs designs. However, this is worth a special investigation that is beyond the scope of this paper.

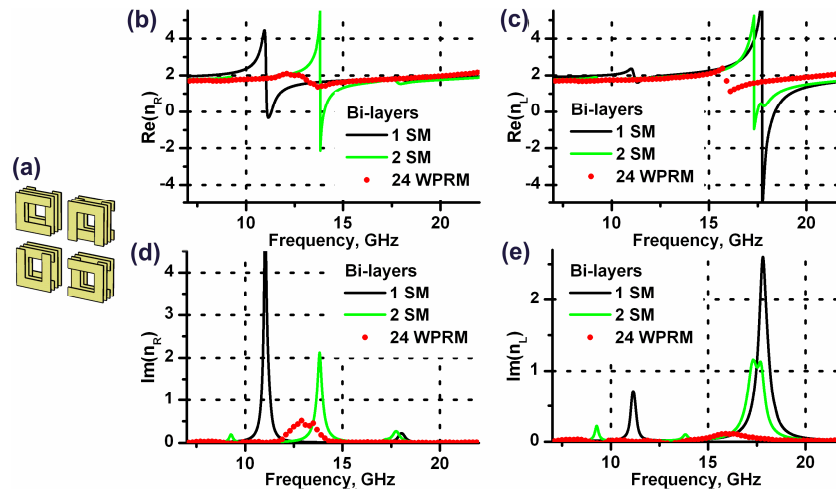


Fig. 5. (Color online). U-shaped MTM design (a). Effective refractive indices of the U-shaped MTM, retrieved with SM (one bi-layer – black line, two bi-layers – green line) and WPRMC (red circles): (b) $Re(n_R)$, (c) $Re(n_L)$, (d) $Im(n_R)$, (e) $Im(n_L)$.

4. Conclusion

In this paper we presented the wave propagation retrieval method for chiral metamaterials. However, the WPRMC is suitable to retrieve bulk effective parameters of any kind of materials with RCP and LCP eigenwaves. The method's validity is verified on the case studies of homogeneous magnetized plasma and bi-cross chiral MTMs. We also analyzed the case of U-shaped MTMs possessing extremely poor convergence of effective parameters with the slab thickness. In such case the WPRMC provides important information on the bulk effective properties which are difficult or even impossible to obtain by the standard method with the few layers structures. Our method is straightforward in implementation and restores effective properties unambiguously. All this make the WPRMC a useful tool in chiral MTMs research.

Acknowledgments

The authors gratefully acknowledge partial support from the Danish Research Council for Technology and Production Sciences via the NIMbus project and thank Prof. C. Simovski for pointing on the problems in the effective impedance restoration.